New inputs on CAI formation based on a new CV3 meteorite Northwest Africa 10261. I. Gyollai[1], A. Kereszturi[2], M. Szabo[1], Zs Kereszty[3] [1]HAS Research Centre for Astronomy and Earth Sciences, Institute for Geology and Geochemistry (gyildi@gmail.com), [2]HAS Research Centre for Astronomy and Earth Sciences, Institute for Astronomy (kereszturiakos@gmail.com), [3]IMCA (cbo@t-online.hu)

Introduction: The meteorite Northwest Africa 10261 (NWA 10261) meteorite was found by nomad in Morocco, and purchased by Zs. Kereszty private collector in 2014. The NWA 10261 meteorite was classified as CV3 chondrite by authors, which were approved by Meteoritical Bulletin in 2016 [1]. The aim of this work is the correlated optical microscopy and SEM-BSE, SEM-EDX analyses of a recently found new meteorite Northwest Africa 10261 (NWA 10261), which shows high abundance of AOA and CAI components, in order to get more insight into the formation of such grains, focusing on their mineral and chemical characteristics with special emphasis on one unique CAI grain.

Methods: For textural analysis a polarization microscope NICON Eclipse E600 POL was used. Infrared spectra were collected with a Bruker VERTEX70 HYPERION 2000 FTIR-ATR microscope (MCT-A detector). The measurements were performed for 30 scans at 4cm^{-1} spectral resolution, with Bruker Optics' Opus 5.5 software. The elemental composition of the measured locations was determined by EPMA with 1–2 µm spatial resolution with vacuum deposited thin amorphous carbon layer on the sample, using a JEOL Superprobe 733 with an INCA Energy 200 Oxford Instrument Energy Dispersive Spectrometer. The analytical circumstances are 20 keV acceleration voltage, 6 nA beam current and count time of 60 s.

Results: In this work we analysed one thin section of NWA 10261 CV3 meteorite, and one CAI grain in it titled J71, which has roughly isometric, amoeboid form of 200 µm diameter (Fig 1). We separated to the following main sections the CAI grain, based on the BSE image: *(A)* Inner, fractured, light and homogeneous area (one 120x60 micrometer sized single garnet-rich grain, with minor melilite and spinel content in its fractures). (*B)* Inner part, surrounding the zone A with dark and light patches of submiscorscopic grain size of (spinel-melilite rich zone). (*C)* Light granular part containing 2-4 micron sized Ca-pyroxene, the grains are larger than the submicroscopic, with melilite-rich grain environment. between these grains patches in which (pyroxene-melilite) . (*D).* Homogeneous layer near to the rim (submicroscopic) pyroxene-melilite. (E) Granular layer (below 0.1-0.5 micrometer sized grains which have fine-grained rim are mainly olivine, fewer pyroxene and melilite.. *F*. Grey, homogeneous layer of pyroxene and melilite (submicroscopic). Among the above mentioned units D, E and F form a layered structure around the inner A and B units. Below we describe the three main mineral types of this CAI: the central garnet, melilites, grossular and spinels, focusing on their similarities and differences compared to the main units. The melilites are very fine grained, neither by optical microscopy and on BSE image could be separated different grains, only in the granular "C" zone could be observed separated isometric grains (2-4 µm) as hole fillings, and in "E" zone such grains rarely observed. Melilites are present in the mid-dark areas around the garnet-rich A-zone, and fills approximately 50% of the CAI.

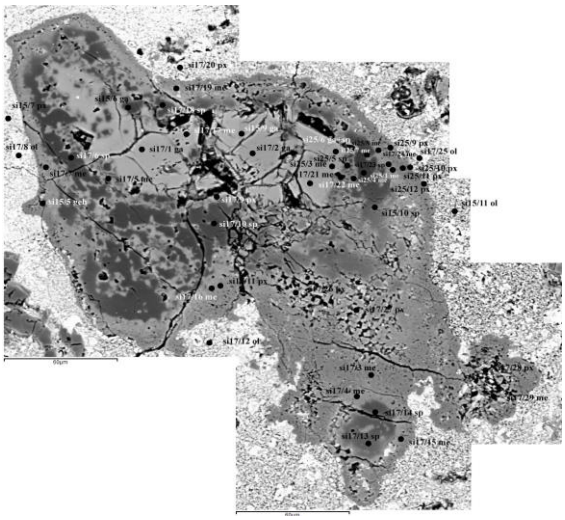

Fig. 1: BSE image with measuring points of J71 CAI.

In the following we compare nearby grains of the same minerals in the same zones to see similarities between them (Fig2).

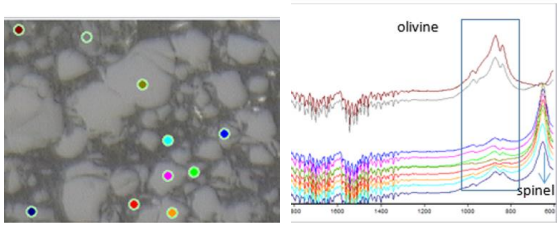

Fig. 2. FTIR spectra of olivine-spinel rich zone olivine has bands near 830 and 860 cm-1, the spinel at 648 cm-1.

The J71 si17/15me+si17/4me (Fig. 1.) melilite pairs (D zone) are very similar to each other, characterized by near 3% TiO_2 and 23-24% CaO, but si17/4 is characterized by a bit lower Al_2O_3 (16.4%) and MgO (10.3%) than si17/15 (18.6%, 12.2%). These melilites are characterized by lower Al_2O_3 content than other melilte in A and B zones, and lower CaO content than melilites in B zone. The FeO content is lower than of other melilites in C zone. Significant difference is obtained in FeO content, the si17/15 has 4.4%, whereas in si17/4 was not detected. This melilite grain pair is characterized by lower Al_2O_3 than average melilite composition of D zone and lower than other zones of inner parts in A, B, C

zones. The si17/13sp+si17/14sp mineral spinel pair (B zone) show more observable difference from each other in composition, only their MgO is similar (20%). The si17/13sp has higher Al_2O_3, (62.8%), FeO (16%), but lower CaO (0.9%), than si17/4me (50.9% Al_2O_3, 9.9% FeO, 4.7% CaO). Other important difference, that si17/4me contain SiO_2 (13%) and TiO_2 (0.6%) whereas the si17/4me not.

Discussion: Based on [2] publication, The reverse zoning of melilite (the higher temperature, Al-melilite (gehlenite)) is at the outer part of CAI, whereas and the lower temperature Mg-rich melilite (akermanite) is at inner part of CAI, what might be explained by direct condensation from a solar nebular gas with decreasing pressure [2] or by crystallization from melt with melt evaporation [3]. The Al-rich melilite (gehnenite) crystallizes at higher temperature than Mg-rich melilite (akermanite) [4]). Indeed, in our case the Al_2O_3 in core zone was the highest which decreased outward in J71 CAI. The Ca content is the highest in the core zone, which decreases outward of the CAI. The Ca is lowest in the spinel-rich B zone implying a particular depletion of the inner part of CAI. These difference in melilites could be observed in our J71 nodule-type CAI where inner part occur Mg-rich melilite (akermanite), whereas Al- rich melilite occur at the rim of CAIs, which indicates a crystallization of CAI higher temperature at rim area. The gehlenite was measured at rim of J71 CAI, and Al-enrichment could be detected at the rims. Alternatively the CAI could be occurred inner, higher temperature part of the solar nebula than during in initiation of crystallization in 1520-1568 K. The presence of gehlenite at the rim of J71 nodule type CAI suggests higher temperature crystallization (1625 K, [5] (in B zone. The mellilite was observed in several cases (C zone) together with Al-Ti rich pyroxenes (fassait/titanoaugite), which propose 1520-1568 K eutectic melting temperature [4]. We detected these coexistence coexistence of mellilite + Ti-augite at the rim of J71 CAI (si17/16 + SI17/11), while [6] studied Mg/Al fractionation of melilites by Al-Mg isotopy method, concluding the Mg/Al fractionation event occurred when the CAI last melted. The higher Al content occurred in the core zone of CAIs (garnet and melilit rich zone) whereas Mg enrichment was observed in spinel rich part of B zone, and forsterite bearing zone in the transition to the matrix (F zone+ forsterite+enstatite).

The garnet rich core zone crystallized between 800-1040 °C, and the condensation temperature increased in B zone between 1515-1625 K, which decreased slightly toward the outer zones 1520-1565 K (C, E zone), and 1475 K (D zone). The Fe-metasomatism of C zone could occurred below 800 °C. Summarily, the J71 CAI shows a cyclic condensation history, with lower condensation temperature in core zone, and higher condensation temperature in the outer zones.

Following [7] the CAI minerals could be distinguished to primary (precursor) – and secondary minerals. The primary CAI minerals are melilit, anorthite, Al-Ti diopside (fassaite/titanoaugite), hibonite, spinel perovskite, grossular. The crystallization temperature of primary CAI minerals analyzed by [5] are the followings: gehlenite 1625 K, spinel 1513, Fe-Ni 1473, diopside 1450 K, forsterite 1444 K, enstatite 1349 K. Alternatively, [8] suggested crystallization temperature for Ti-Al rich pyroxene 1550 K, akermanite 1475 K, wollastonite 1450 K. Secondary minerals, which were observed in our AOAs and CAIs are grossular, andradite, hedenbergite, wollastonite, olivine, ferroan spinel, diopside, smectite. The garnet rich core formed between 800-1040 °C, the cryptocrystalline melilite in the fractures formed at 1600 K proposed higher temperature alteration of J71 CAI. Grossular occurs rather only in the inner part in the J71, there could be interpreted as primary, lower temperature condensate (below 800 °C,) [5]. However, the garnets in the rims of AOAs crystallized at lower temperature (below 800°C) than the forsterites (1444 K) in the inner part, proposing slow cooling of AOA [5].

Conclusion Summerizely, by chemical-mineralogical mapping of J7-1 in NWA 10261 CV3 meteorite, the **condensation history** could be reconstructed by temperature: 1. crystallization of core zone between 800-1040 °C (A zone); 2. spinel-melilit rich inner rim between 1513-1625 K (B zone); 3. mellilite + fassaite at 1528 K, which followed by Fe-metasomatism below 800 K (C zone); kaermanite formation at 1475 K (D zone) ; mellilite, fassaite, diopide 1450 -1568 K (E zone) ; FeNi, forsterite, diopside, enstatite (F zone) 1443-1473 K. Based on publications Fe-metasomatosis of CAIs occurs when the nebula become more oxidizing and temperature decreases belong 800 °C (Grossman, 1975), which is observed in our Fe-riche (pleonast) spinel in J7-1 CAIs.

Acknowledgement: The microprobe measurements were supported by the GINOP 2.3.2-15-2016-00009, the other parts of the meteorite analysis in general was supported by the GINOP-2.3.2-15-2016-00003 fund of NKFIH.

References: [1] Bouvier, A., Gattacceca, J., Grossman, J. and Metzler, K., 2017. The Meteoritical Bulletin, No. 105. Meteoritics and Planetary Science, 52, pp.2411-2411. [2] Macpherson, G. J., & Grossman, L. (1984). GCA, 48(1), 29-46. [3] Grossman, L., Ebel, D. S., & Simon, S. B. (2002). GCA, 66(1), 145-161. [4] Kawasaki, N., Sakamoto, N., & Yurimoto, H. (2012). MAPS, 47(12), 2084-2093, [5] Blander, M., & Fuchs, L. H. (1975). GCA, 39(12), 1605-1619., [6] MacPherson, G. J., Kita, N. T., Ushikubo, T., Bullock, E. S., & Davis, A. M. (2012). EPSL 331, 43-54., [7] Krot, A. N., Scott, E. R., & Zolensky, M. E. (1995). Meteoritics, 30(6), 748-775., [8] Grossman, L. (1975). GCA, 39(4), 433-454.